

Chapter 2

Iron Rich Iron-Aluminides

Over the 80 years of research on iron-aluminides immense amount of literature was produced. This chapter summarizes some of the relevant prior work. First, the Fe–Al phase diagram and ideal equilibrium structures of Fe–Al compounds are described. Next, the defects; vacancies, anti-site atoms, dislocations and anti-phase boundaries (APBs) important in the real materials are covered. Finally the yield stress anomaly is discussed. Of course there exists much more information on Fe–Al system, however it can not possibly be all covered in this review.

2.1 Structure

The aluminum rich half of the iron–aluminium phase diagram (Fig. 2.1) contains several intermetallic compounds: $\text{Al}_{13}\text{Fe}_4$, Al_5Fe_2 , Al_2Fe and high temperature ε - Al_8Fe_5 . These compounds have often quite complicated structures: Al_2Fe is triclinic with $\text{P}\bar{1}$ symmetry and 19 atoms/unit cell [12], monoclinic $\text{Al}_{13}\text{Fe}_4$ with 102 atoms/unit cell approximates decagonal quasicrystal [3, 24] and orthorhombic Al_5Fe_2 features Al atoms moving almost freely inside pentagonal channels [6, 60]. High temperature ε - Al_8Fe_5 was only recently determined to be Hume-Rothery Cu_5Zn_8 -type (52 atoms/unit cell, Strukturbericht symbol $\text{D}8_2$) [86].

The iron rich part of phase diagram is dominated by bcc based compounds with varying degree of order (Sect. 2.1.2) depending on temperature and composition [5]. The maximum solubility of aluminium in the high temperature fcc γ -iron is only about 1.5 at.% [88].

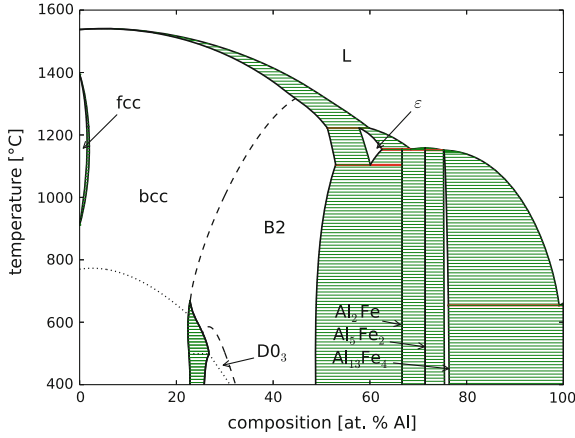


Fig. 2.1 Fe–Al phase diagram according to Sundman et al. [88]. *Black* zero phase fraction lines, *green* tie lines, *red* invariant equilibria, *dotted* ferromagnetic transitions, *dashed* order-disorder transitions

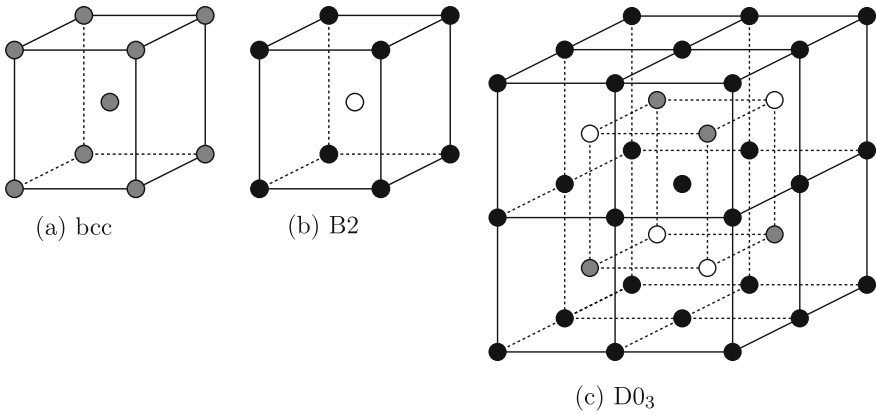
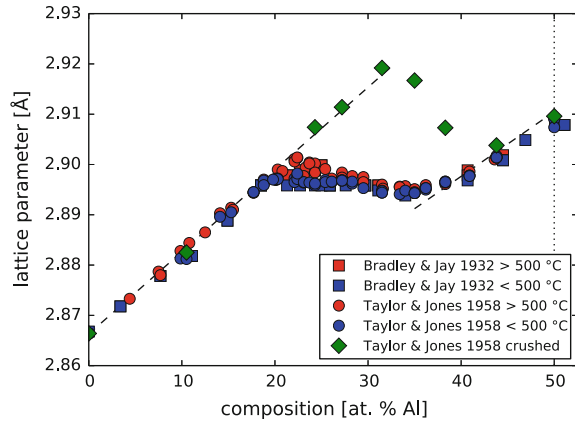


Fig. 2.2 Unit cells of bcc, B2, and D0₃ structures. *Black*, *white* and *gray* circles indicate differently occupied sites

The bcc structure (α -iron, Strukturbericht symbol A2) contains two equivalent positions in the middle and in the corner of the cubic cell (Fig. 2.2a). In the B2 structure¹ these two sites are occupied differently (Fig. 2.2b). D0₃ structure has space-group $Fm\bar{3}m$ and three non-equivalent lattice sites at Wyckoff positions 4a, 4b and 8c (Fig. 2.2c). At ideal 3:1 stoichiometry it is a superstructure of alternating bcc and B2 cells. The smallest unit cell corresponds to a $2 \times 2 \times 2$ stack of 4 bcc and 4 B2 unit cells.

¹In older literature [26, 89] L2₀ symbol is used instead of B2 [35].

Fig. 2.3 Lattice parameter of Fe–Al alloys [5, 91]



2.1.1 Lattice Parameter

The room temperature lattice parameter (Fig. 2.3) of bcc cell increases linearly with aluminium content from 0.28664 nm for pure iron to about 0.2895 nm at 18 at.% Al. Beyond this composition the linear increase continues only for disordered alloys (either quenched from higher temperature or heavily cold worked) [91]. For equilibrium alloys beyond 18 at.% Al the lattice parameter stays in 0.2894–0.2897 nm range with indistinct local minima and maxima indicating the phase boundaries. The lattice parameter of $D0_3$ superstructure is twice the given value. Beyond about 33 at.% Al in the B2 region the lattice parameter rises again to a maximum value of 0.2909 nm for stoichiometric FeAl. For hyper-stoichiometric FeAl alloys the lattice parameter decreases with excess Al content [10] indicating the triple-defect type of defect structure. Since the lattice parameter of quenched alloys is directly related to the vacancy content, it was measured in almost every work quoted in the section on vacancies (Sect. 2.2.1).

2.1.2 Long-Range Order and Sublattice Occupancies

Perfectly ordered $D0_3$ and B2 structures with sublattices fully occupied by their native species correspond to 3:1 and 1:1 stoichiometric compositions. The influence of temperature and deviations of composition from stoichiometry on the occupation of sublattices was studied using X-ray [5, 14, 26, 46, 55, 67, 100] and neutron [29, 40, 103] diffraction. The sublattice occupancies are usually characterized by (long-range) order parameters. However, every researcher uses “slightly different definition” [40]. Therefore, the general features of order in Fe–Al system are illustrated in the Fig. 2.4 directly using the sublattice occupancies.

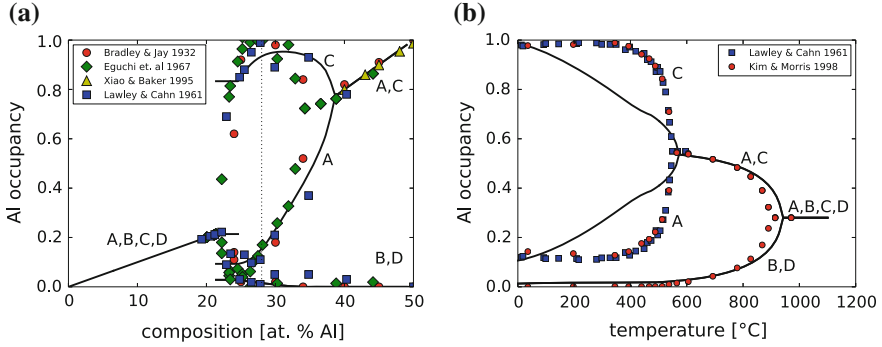


Fig. 2.4 Variation of sublattice occupancies with composition (a) and temperature (b). *Full lines* are calculated from the model of Sundman et al. [88]. Data are taken from Bradley and Jay [5], Taylor and Jones [91], Eguchi et al. [14], Morris and Kim [40] and Xiao and Baker [100]. Temperature variation is shown for 28 at. % Al indicated by a dotted vertical line on the composition plot. Data for composition dependence are for slowly cooled alloys. Sundman’s model was evaluated at 400 K

Let us describe the $D0_3$ unit cell as 4 interlocking fcc (sub)lattices (labeled A, B, C and D) each displaced from the previous by $\frac{1}{4}[111]$. In the bcc region of the phase diagram the occupancy of all four sublattices is the same and equal to the overall alloy composition ($x_{A,B,C,D}^{Al} = x^{Al}$). In the sub-stoichiometric B2 alloys ($x^{Al} < 0.5$) at low temperatures one pair of sublattices is occupied almost exclusively by iron ($x_{B,D}^{Al} = 0$), and the other pair contains mixture of the excess iron and aluminium ($x_{A,C}^{Al} = 2x^{Al}$). As the temperature approaches the transition to bcc the differences in occupancies of sublattices continuously diminish. For aluminium rich B2 alloys the situation is complicated by so called “constitutional” vacancies. For more details see the Sect. 2.2.1. $D0_3$ alloys similarly to B2 alloys have a pair of iron sublattices ($x_{B,D}^{Al} = 0$), but the occupancies of sublattices A and C differ. Again these differences continuously diminish with the temperature approaching the B2 transition.

2.1.3 Phase Transformations

Transformations between $D0_3$ and B2 and between B2 and bcc (indicated by dashed lines in Fig. 2.1) are higher than first order. They are characterized by continuous change in the order parameter (sublattice occupancies), no region of phase coexistence and no latent heat. Critical exponent² $\beta = 0.307$ for transformation between $D0_3$ and B2 differs from the value obtained from Landau’s theory $\beta = 0.5$ and seems to match the value for Ising model [26]. The λ transition line between bcc and B2 ends at the tricritical point, below which a miscibility gap is present in the Fe–Al

² Long-range order parameter below the critical temperature is proportional to $(T_C - T)^\beta$.

system. This results in a two-phase bcc + B2 and bcc + D0₃ regions in the phase diagram. X-ray and neutron diffraction can determine only the macroscopic averages of sublattice occupancies and thus do not give the complete picture in the case of two-phase microstructure [14]. Morphology of the microstructure in the two-phase region was therefore studied by TEM [56, 73, 78, 89]. Allen and Cahn [1] related the observed microstructure to the thermodynamic principles of phase separation and Ikeda et al. [33] used diffusion couple specimens to cover whole composition range of two-phase region in their thorough work.

2.1.4 Short-Range Order and K-State

In the composition range from 10 to 20 at.% Al, the Fe–Al alloys annealed at low temperature ($\approx 300^\circ\text{C}$) after being quenched from high temperature ($\approx 800^\circ\text{C}$) exhibit curious increase of resistivity [79, 92] and contraction on dilatometry [13] along with other anomalies indicating presence of a different phase. X-ray diffraction shows diffuse intensity maxima appearing at the places of D0₃ superstructure reflections [13, 15, 16]. That would indicate short-range order [16, 32, 61, 71], or long-range order with very small antiphase domains [13, 15]. TEM study [97] found two-phase bcc + D0₃ microstructure with very small D0₃ particles. It has been suggested [13, 97] that the formation of ordered state is facilitated by excess vacancies quenched from high temperature. The X-ray study of Taylor and Jones [91] mentions Fe₁₃Al₃ phase in this region, however it was not confirmed by other researchers [15, 97]. Becker and Schweika observed ferromagnetically stabilized B32 order in this region [4, 83]. B32 order was observed during bcc to D0₃ transition [21] as well. Recently Ikeda et al. [33] determined boundary between bcc and bcc + D0₃ two-phase region to extend at low temperatures to much lower Al concentrations than previously thought. This extended bcc + D0₃ two-phase field thus covers part of the area where “K-state” anomalies were observed. In the rest of the region short-range order may be still responsible for the anomalies.

2.2 Defects

2.2.1 Point Defects: Vacancies and Anti-site Atoms

The perfectly ordered state can be realized only at the stoichiometric composition and at 0 K. The off-stoichiometric composition as well as entropy requirements at higher temperatures are satisfied by point defects (vacancies and anti-site atoms).

Historically two classes of B2 compounds were distinguished [11], depending on how the deviations from perfect 1:1 stoichiometry are accommodated. In the anti-site defect compounds anti-site atoms accommodate the composition on both sides of

stoichiometry. In the triple defect compounds, on the one side of the stoichiometry the composition is matched by anti-site atoms, while on the other side, excess atoms are matched by vacancies on the other sublattice. These vacancies, present in great amounts determined by the composition, were called constitutional vacancies since they were thought to persist in the material all the way down to 0 K. Thermally created defects in the anti-site defect compounds are pairs of anti-site atoms. In triple defect compounds it is a pair of vacancies and an anti-site atom—a triple defect.

FeAl was considered to be a triple defect compound, with Fe anti-site atoms in Fe rich alloys and Fe vacancies in Al rich alloys. The presence of vacancies in Al rich alloys is indicated by the linear decrease of lattice parameter beyond 50 at.% Al [70].

For triple defect compounds Neumann et al. [66] suggested simple model describing the variations of defect concentration with composition:

$$z^2(z - 2\chi) = \alpha^3, \quad \alpha = Ae^{\frac{B}{T}}, \quad (2.1)$$

where z is the vacancy concentration, χ is the deviation of composition from stoichiometry and α is the vacancy concentration at stoichiometry. This model is based on the assumption that the concentration of minority defects—Al vacancies and Al anti-site atoms—is zero.

The match between this model and experimentally determined vacancy concentrations is rather good (Fig. 2.5), especially if we consider different conditions of alloys investigated by different researchers and the error in the determination of vacancy concentration.

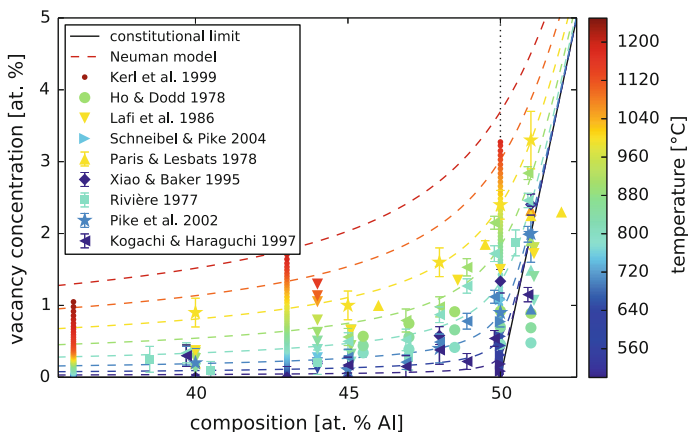


Fig. 2.5 Compilation of vacancy concentration measurements [31, 36, 41, 54, 68, 69, 76, 82, 100]. Solid black line shows the amount of constitutional vacancies. Colour dashed lines show vacancy concentration calculated from Neumann model (2.1) with $A = 0.57$ and $B = -4050$ K as fitted to the data of Pike et al. [69] for stoichiometric FeAl at 700 and 1000 °C

Additionally Neumann [65] tried to sort out various B2 compounds into the anti-site defect and triple defect classes based on their enthalpy of formation. Strongly ordered compounds with high enthalpy of formation belong to the triple defect class and weakly ordered compounds with low enthalpy of formation belong to the anti-site defect class. FeAl, however, ends up somewhere in the middle of the range. This led to the abandoning of the idea of two distinct classes of B2 compounds in favour of the hybrid models [27, 37–39, 44, 45, 49, 50] that describe whole spectrum of the behaviour between purely anti-site defect and purely triple defect limits. These models take into account non-zero concentration of all four kinds of defects. Several of these more rigorously derived models question the existence of constitutional vacancies [38, 39, 45, 72] and propose that FeAl and other B2 compounds accommodate the deviations from stoichiometry by anti-site atoms on both sides of stoichiometry with no vacancies at 0 K. As the concentration of thermal vacancies increases with temperature, Al anti-site atoms can recover to their original sublattice. Experimentally observed vacancy concentration is due to the frozen-in thermal vacancies, since the diffusion practically stops before 0 K base state is reached. Recovery of anti-site atoms was observed by Kogachi and Haraguchi in their neutron [47] and X-ray [43] diffraction experiments coupled with vacancy concentration measurements [41]. Diffraction experiments on their own can not precisely and uniquely determine the vacancy content, therefore they measured the vacancy content independently and used diffraction data only to determine the distribution of these vacancies between the two sublattices. They claimed appreciable concentration of Al vacancies what created a bit of a controversy [17, 42]. Their other conclusions however stay sound. Notably the total vacancy concentration lower than constitutional limit supports the idea of nonexistence of constitutional vacancies. Moreover, they argued that older measurements of the vacancy concentration might have been affected by voids present in the bulk material that lower the density and thus artificially inflate the measured vacancy content. Themselves, they avoided this source of error by using powder for density measurements.

In pure metals the concentration of vacancies increases with temperature according the Arrhenius law [18]:

$$c_V(T) \propto e^{\frac{-H_V}{k_B T}}, \quad (2.2)$$

where H_V is vacancy formation enthalpy and k_B is Boltzmann constant. In (partially ordered) alloys the energetics of vacancy formation depends on a particular atomic arrangement around the defect [36]. For example, strong tendency for formation of divacancies and vacancy clusters was found in ab-initio calculations [20]. Moreover, different kinds of defects (vacancies and anti-site atoms) have to coexist [18]. Therefore, the enthalpies of formation obtained from Arrhenius plots have to be regarded as effective values [18, 36]. These effective vacancy formation enthalpies can be determined by various indirect methods such as resistometry [74, 75], calorimetry [54], time-differential length change measurements [80] and positron annihilation spectroscopy [81, 98]. Values summarized in [34, 36] scatter widely around 1 eV with almost no systematic dependence on composition. Ab-initio calculations give

similar values [18–20]. Kerl [36] measured the temperature evolution of absolute vacancy concentration using dilatometry and found changes in the slope of Arrhenius plot corresponding to the tentative phase boundaries given in the phase diagram of Kubaschewski [52]. These boundaries were based on the work of Köster and Gödecke [48] however their nature is unclear. Recently a cluster-variation based model that takes into account local correlations (short-range order) by considering $3^9 = 19683$ kinds of differently occupied cubic clusters was proposed by Semenova et al. [84].

2.2.2 Dislocations

Dislocations are linear defects in the material. Volterra [96] first studied dislocations as topological defects in elastic solids. If an elastic solid is cut, two sides of the cut displaced and then reconnected, then dislocation is a boundary of that cut. The displacement is called Burgers vector (\mathbf{b}) and is a basic characteristic of a dislocation. In crystalline material, possible Burgers vectors of dislocations are restricted by the crystal lattice. Energy of a dislocation is proportional to b^2 , therefore only the smallest lattice displacements are stable. In particular in bcc structure it is $\mathbf{b} = 1/2\langle 111 \rangle$ and $\langle 100 \rangle$ [30].

The motion of dislocations under stress is responsible for plastic yielding of materials. The stress needed to move a dislocation is called Peierls stress. At low temperatures dislocations glide only under stresses higher than Peierls stress. At higher temperatures, thermal fluctuations lead to creation of kinks and dislocation can move by kink migration [7, 90]. This is the case of bcc $\mathbf{b} = 1/2\langle 111 \rangle$ screw dislocations since their Peierls stress is particularly high because their core is supposed to be split on multiple planes [94, 95].

In B2 structure the $\mathbf{b} = 1/2\langle 111 \rangle$ dislocation creates an anti-phase boundary (Sect. 2.2.3). A pair of $\mathbf{b} = 1/2\langle 111 \rangle$ dislocations is needed to restore the chemical order. The two dislocations joined by an APB stay at equilibrium distance since the repulsion force between them is countered by the energy of the APB.

In DO_3 structure the situation is even more complicated: Four $1/4\langle 111 \rangle$ dislocations (equivalent to $\mathbf{b} = 1/2\langle 111 \rangle$ in bcc due to double lattice parameter) are needed to restore the order and two different kinds of APB are formed between them (Fig. 2.6, Sect. 2.2.3) [51, 57]. Energy of DO_3 APB is small (since it affects only the second nearest neighbours) and often the two pairs are quite separated or only one pair with trailing DO_3 APB is observed [77].

Fig. 2.6 Structure of perfect superdislocation in DO_3 lattice



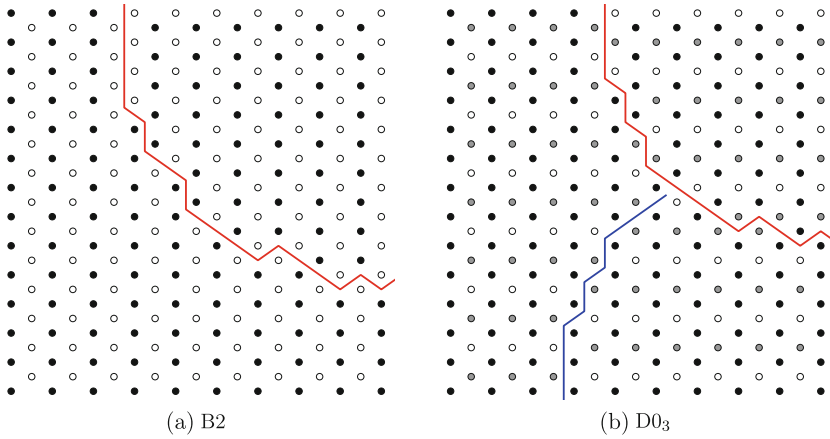


Fig. 2.7 (110) planes of B2 and D0₃ structures. In both structures B2 APB is shown and highlighted in *red*. Additionally in D0₃ structure D0₃ APB is shown and highlighted in *blue*

2.2.3 Anti-phase Domains and Boundaries

Anti-phase domain is a region with homogeneous chemical order. It is typically created by the growth of an initial ordered nucleus. When two such growing domains collide the order developed in each of them might have different origin. In that case an anti-phase domain boundary (APB) is formed between them. APB is a planar defect similar to a stacking fault, however across the APB the crystal lattice remains geometrically intact and only the chemical order is affected.

Different states of order found in Fe–Al alloys give rise to different anti-phase domain structures [58]. In the case of B2 order the APB is characterized by $\frac{1}{2}[111]$ displacement and affects nearest neighbour bonds (Fig. 2.7a). In the D0₃ structure this boundary is characterized by $\frac{1}{4}[111]$ displacement due to the double lattice parameter of D0₃ structure. Additional kind of APBs specific to D0₃ structure affects next nearest bonds and is characterized by $\frac{1}{2}[111]$ or $\frac{1}{2}[100]$ displacements (Fig. 2.7b).

APBs created on the interface between growing nuclei of ordered structure during ordering transformation are called thermal APBs. APBs are created also behind moving imperfect dislocations (Sect. 2.2.2). These are called deformation APBs.

2.3 Yield Stress Anomaly

Strength of bcc metals decreases monotonously with increasing temperature as the thermally activated nucleation of kinks on $\frac{1}{2}[111]$ screw dislocations becomes more efficient [90]. Curiously though, ordered Fe–Al alloys exhibit a temperature range where their yield stress increases with temperature. This gives rise to a peak in the

yield stress occurring at about 800 K [101]. In B2 alloys, this peak was discovered only in the 1990s [9, 25, 99] since it is often masked by strengthening due to excess vacancies [8].

In $D0_3$ Fe–Al alloys the peak temperature corresponds well to the $D0_3 \leftrightarrow B2$ transition. This motivated the attempts of Stoloff and Davies [87] to explain the yield stress anomaly (YSA) by the change of deformation mechanism from motion of super-dislocations to motion of single dislocations related to the gradual loss of order. Nevertheless, this can not explain the peak observed in B2 alloys. Moreover, Stein et al. [85] investigated quaternary Fe–Al₂₆–Ti₄–X₂ (X = V, Cr, Nb, Mo) alloys and found that although alloying shifted the $D0_3 \leftrightarrow B2$ transition temperature, the YSA peak temperature remained unaffected. Thus, there seems to be no correlation between the stress anomaly and the degree of ordering.

Slip transition from $\langle 111 \rangle$ to $\langle 100 \rangle$ slip was observed at the temperature of YSA peak [2, 59, 93, 102]. The change of a slip system can be explained by hardening of the $\langle 111 \rangle$ slip until $\langle 100 \rangle$ slip is easier [102]. Drop of the yield stress after the peak is then caused by the rapid softening of $\langle 100 \rangle$ slip.

Quite a few mechanisms were suggested as an explanation of hardening of $\langle 111 \rangle$ system: Morris and Morris [62] reviewed several mechanisms based on the thermally activated locking of dislocations: cross-slip pinning, local climb locking, pinning by APB relaxation, change of slip plane, ... George and Baker [22] proposed that “the yield stress increase with increasing temperature is a result of the solid-solution hardening due to thermal vacancies”. Moreover, their measurements [23] revealed that yield stress depends on the time samples are kept at deformation temperature before the test and that the yield stress of quenched samples tested at room temperature matches the yield stress of samples deformed at elevated temperature. This is consistent with vacancy hardening as vacancies need time to reach equilibrium concentration when the temperature is changed and their concentration can be retained by quenching. On the other hand these observations are inconsistent with thermally activated processes affecting motion of dislocations at elevated temperature directly [63]. The issue, though, remains unsettled. Articles were published recently both supporting [28, 64] and questioning [53] the vacancy hardening explanation of YSA.

References

1. S.M. Allen, J.W. Cahn, Mechanisms of phase transformations within the miscibility gap of Fe-rich Fe–Al alloys. *Acta Metall.* **24**(5), 425–437 (1976). doi:[10.1016/0001-6160\(76\)90063-8](https://doi.org/10.1016/0001-6160(76)90063-8)
2. I. Baker, D.J. Gaydos, Flow and fracture of Fe–Al. *Mater. Sci. Eng.* **96**, 147–158 (1987). doi:[10.1016/0025-5416\(87\)90549-0](https://doi.org/10.1016/0025-5416(87)90549-0)
3. J.-N. Barbier, N. Tamura, J.-L. Verger-Gaugry, Monoclinic Al₁₃Fe₄ approximant phase: a link between icosahedral and decagonal phases. *J. Non-Cryst. Solids* **153**(154), 126–131 (1993). doi:[10.1016/0022-3093\(93\)90328-U](https://doi.org/10.1016/0022-3093(93)90328-U)
4. M. Becker, W. Schweika, B32 order in iron rich Fe–Al alloys. *Scr. Mater.* **35**(11), 1259–1264 (1996). doi:[10.1016/1359-6462\(96\)00311-9](https://doi.org/10.1016/1359-6462(96)00311-9)

5. A.J. Bradley, A.H. Jay, The formation of superlattices in alloys of iron and aluminium. *Proc. R. Soc. Lond. Ser. A* **136**(829), 210–232 (1932). doi:[10.1098/rspa.1932.0075](https://doi.org/10.1098/rspa.1932.0075)
6. U. Burkhardt et al., Structure reinement of the iron-aluminium phase with the approximate composition Fe_2Al_5 . *Acta Crystallogr. Sect. B Struct. Sci.* **50**(3), 313–316 (1994). doi:[10.1107/S0108768193013989](https://doi.org/10.1107/S0108768193013989)
7. W. Cai et al., Kinetic Monte Carlo modeling of dislocation motion in BCC metals. *Mater. Sci. Eng. A* **309–310**(0), 270–273 (2001). doi:[10.1016/S0921-5093\(00\)01689-0](https://doi.org/10.1016/S0921-5093(00)01689-0)
8. R. Carleton, E.P. George, R.H. Zee, Effects of deviations from stoichiometry on the strength anomaly and fracture behavior of B-doped FeAl. *Intermetallics* **3**(6), 433–441 (1995). doi:[10.1016/0966-9795\(94\)00041-1](https://doi.org/10.1016/0966-9795(94)00041-1)
9. K.M. Chang, Tensile and impact properties of directionally solidified Fe-40Al intermetallic. *Metall. Trans. A* **21–11**, 3027–3028 (1990). doi:[10.1007/BF02647223](https://doi.org/10.1007/BF02647223)
10. Y.A. Chang et al., Correlation of the hardness and vacancy concentration in FeAl. *Intermetallics* **1**(2), 107–115 (1993). doi:[10.1016/0966-9795\(93\)90028-T](https://doi.org/10.1016/0966-9795(93)90028-T)
11. Y.A. Chang, J.P. Neumann, Thermodynamics and defect structure of intermetallic phases with the B2 (CsCl) structure. *Prog. Solid State Chem.* **14**(4), 221–301 (1982). doi:[10.1016/0079-6786\(82\)90004-8](https://doi.org/10.1016/0079-6786(82)90004-8)
12. I. Chumak, K.W. Richter, H. Ehrenberg, Redetermination of iron dialuminide, FeAl_2 . *Acta Crystallogr. Sect. C Cryst. Struct. Commun.* **66**(9), i87–i88 (2010). doi:[10.1107/S0108270110033202](https://doi.org/10.1107/S0108270110033202)
13. R.G. Davies, An X-ray and dilatometric study of order and the "K-state" in iron-aluminum alloys. *J. Phys. Chem. Solids* **24**(8), 985–992 (1963). doi:[10.1016/0022-3697\(63\)90002-7](https://doi.org/10.1016/0022-3697(63)90002-7)
14. T. Eguchi et al., Order-disorder transformation in Fe-Al alloys. *Trans. Jpn. Inst. Met.* **8**, 174 (1967)
15. J.E. Epperson, J.E. Spruiell, An X-ray single crystal investigation of iron-rich alloys of iron and aluminum-I. Phase relations in alloys containing between 14 and 23 at.% aluminum. *J. Phys. Chem. Solids* **30**(7), 1721–1732 (1969). doi:[10.1016/0022-3697\(69\)90240-6](https://doi.org/10.1016/0022-3697(69)90240-6)
16. J.E. Epperson, J.E. Spruiell, An X-ray single crystal investigation of iron-rich alloys of iron and aluminum-II. Difuse scattering measurements of short-range order in alloys containing 14.0 and 18.3 at.% aluminum. *J. Phys. Chem. Solids* **30**(7), 1733–1744 (1969). doi:[10.1016/0022-3697\(69\)90241-8](https://doi.org/10.1016/0022-3697(69)90241-8)
17. M. Fähnle, B. Meyer, G. Bester, Comment on "Point defect behavior in high temperature region in the B2-type intermetallic compound FeAl" by M. Kogachi, T. Haraguchi and S. M. Kim. *Intermetallics* **7**(11), 1307–1308 (1999). doi:[10.1016/S0966-9795\(99\)00052-7](https://doi.org/10.1016/S0966-9795(99)00052-7)
18. M. Fähnle, J. Mayer, B. Meyer, Theory of atomic defects and diffusion in ordered compounds, and application to B2-FeAl. *Intermetallics* **7**(3–4), 315–323 (1999). doi:[10.1016/S0966-9795\(98\)00116-2](https://doi.org/10.1016/S0966-9795(98)00116-2)
19. C.L. Fu, Origin of ordering in B2-type transition-metal aluminides: comparative study of the defect properties of PdAl, NiAl, and FeAl. *Phys. Rev. B* **52**(5), 3151–3158 (1995). doi:[10.1103/PhysRevB.52.3151](https://doi.org/10.1103/PhysRevB.52.3151)
20. C.L. Fu et al., Equilibrium point defects in intermetallics with the B2 structure: NiAl and FeAl. *Phys. Rev. B* **48**(9), 6712–6715 (1993). doi:[10.1103/PhysRevB.48.6712](https://doi.org/10.1103/PhysRevB.48.6712)
21. Z.Q. Gao, B. Fultz, Transient B32-like order during the early stages of ordering in undercooled Fe_3Al . *Phil. Mag. Part B* **67**(6), 787–800 (1993). doi:[10.1080/13642819308219325](https://doi.org/10.1080/13642819308219325)
22. E.P. George, I. Baker, A model for the yield strength anomaly of Fe-Al. *Philos. Mag. A* **77**(3), 737–750 (1998). doi:[10.1080/01418619808224080](https://doi.org/10.1080/01418619808224080)
23. E. George, I. Baker, Thermal vacancies and the yield anomaly of FeAl. *Intermetallics* **6**(7–8), 759–763 (1998). doi:[10.1016/S0966-9795\(98\)00063-6](https://doi.org/10.1016/S0966-9795(98)00063-6)
24. J. Grin et al., Refinement of the $\text{Fe}_4\text{Al}_{13}$ structure and its relationship to the quasihomological homeotypical structures. *Zeitschrift für Kristallographie* **209**(6), 479–487 (1994). doi:[10.1524/zkri.1994.209.6.479](https://doi.org/10.1524/zkri.1994.209.6.479)
25. J.T. Guo et al., Discovery and study of anomalous yield strength peak in FeAl alloy. *Scr. Metall. Mater.* **29**(6), 783–785 (1993). doi:[10.1016/0956-716X\(93\)90226-1](https://doi.org/10.1016/0956-716X(93)90226-1)

26. L. Guttman, H.C. Schnyders, G.J. Arait, Variation of long-range order in Fe₃Al near its transition temperature. *Phys. Rev. Lett.* **22**(11), 517–519 (1969). doi:[10.1103/PhysRevLett.22.517](https://doi.org/10.1103/PhysRevLett.22.517)
27. T. Haraguchi, M. Kogachi, Point defect behavior in B2-type intermetallic compounds. *Mater. Sci. Eng. A* **329–331**(0), 402–407 (2002). doi:[10.1016/S0921-5093\(01\)01613-6](https://doi.org/10.1016/S0921-5093(01)01613-6)
28. G. Hasemann et al., Vacancy strengthening in Fe₃Al iron aluminides. *Intermetallics* **54**, 95–103 (2014). doi:[10.1016/j.intermet.2014.05.013](https://doi.org/10.1016/j.intermet.2014.05.013)
29. K. Hilfrich et al., Phase diagram, superlattices and antiphase domains of Fe₃Al_x, 0.75 ≤ x ≤ 1.3, investigated by neutron scattering. *Acta Metall. Mater.* **42**(3), 731–741 (1994). doi:[10.1016/0956-7151\(94\)90270-4](https://doi.org/10.1016/0956-7151(94)90270-4)
30. J.P. Hirth, J. Lothe, *Theory of Dislocations* (Krieger Pub. Co., 1982)
31. K. Ho, R.A. Dodd, Point defects in FeAl. *Scr. Metall.* **12**(11), 1055–1058 (1978). doi:[10.1016/0036-9748\(78\)90024-8](https://doi.org/10.1016/0036-9748(78)90024-8)
32. C.R. Houska, B.L. Averbach, Atom arrangements in some iron-aluminium solid solutions. *J. Phys. Chem. Solids* **23**(12), 1763–1769 (1962). doi:[10.1016/0022-3697\(62\)90215-9](https://doi.org/10.1016/0022-3697(62)90215-9)
33. O. Ikeda et al., Phase equilibria and stability of ordered BCC phases in the Fe-rich portion of the Fe-Al system. *Intermetallics* **9**(9), 755–761 (2001). doi:[10.1016/S0966-9795\(01\)00058-9](https://doi.org/10.1016/S0966-9795(01)00058-9)
34. J.L. Jordan, S.C. Deevi, Vacancy formation and effects in FeAl. *Intermetallics* **11**(6), 507–528 (2003). doi:[10.1016/S0966-9795\(03\)00027-X](https://doi.org/10.1016/S0966-9795(03)00027-X)
35. A.A. Kelly, K.M. Knowles *Crystallography and Crystal Defects* (Wiley, 2012)
36. R. Kerl, J. Wolf, T. Hehenkamp, Equilibrium vacancy concentrations in FeAl and FeSi investigated with an absolute technique. *Intermetallics* **7**(3–4), 301–308 (1999). doi:[10.1016/S0966-9795\(98\)00118-6](https://doi.org/10.1016/S0966-9795(98)00118-6)
37. S.M. Kim, Vacancy formation in ordered stoichiometric bcc alloys. *Phys. Rev. B* **29**(4), 2356–2358 (1984). doi:[10.1103/PhysRevB.29.2356](https://doi.org/10.1103/PhysRevB.29.2356)
38. S.M. Kim, Vacancies in CsCl-type intermetallic compounds: structural versus thermal. *Phys. Rev. B* **33**(2), 1509–1511 (1986). doi:[10.1103/PhysRevB.33.1509](https://doi.org/10.1103/PhysRevB.33.1509)
39. S.M. Kim, Vacancy properties in ordered CoGa and FeAl. *J. Phys. Chem. Solids* **49**(1), 65–69 (1988). doi:[10.1016/0022-3697\(88\)90136-9](https://doi.org/10.1016/0022-3697(88)90136-9)
40. S.M. Kim, D.G. Morris, Long range order and vacancy properties in Al-rich Fe₃Al and Fe₃Al(Cr) alloys. *Acta Mater.* **46**(8), 2587–2602 (1998). doi:[10.1016/S1359-6454\(97\)00464-3](https://doi.org/10.1016/S1359-6454(97)00464-3)
41. M. Kogachi, T. Haraguchi, Quenched-in vacancies in B2-structured intermetallic compound FeAl. *Mater. Sci. Eng. A* **230**(1–2), 124–131 (1997). doi:[10.1016/S0921-5093\(97\)00016-6](https://doi.org/10.1016/S0921-5093(97)00016-6)
42. M. Kogachi, Reply to comment on "Point defect behavior in high temperature region in the B2-type intermetallic compound FeAl" by M. Fahnle, B. Meyer and G. Bester. *Intermetallics* **7**(11), 1309–1311 (1999). doi:[10.1016/S0966-9795\(99\)00053-9](https://doi.org/10.1016/S0966-9795(99)00053-9)
43. M. Kogachi, T. Haraguchi, Random vacancy distribution in B2-type intermetallic compound FeAl. *Scr. Mater.* **39**(2), 159–165 (1998). doi:[10.1016/S1359-6462\(98\)00145-6](https://doi.org/10.1016/S1359-6462(98)00145-6)
44. M. Kogachi, T. Haraguchi, Possibilities of random vacancy distribution and antisite atom recovering in the point defect mechanism in B2-type intermetallics. *Intermetallics* **7**(9), 981–993 (1999). doi:[10.1016/S0966-9795\(99\)00006-0](https://doi.org/10.1016/S0966-9795(99)00006-0)
45. M. Kogachi, T. Haraguchi, Point defects in B2-type intermetallic compounds. *Mater. Sci. Eng. A* **312**(1–2), 189–195 (2001). doi:[10.1016/S0921-5093\(00\)01892-X](https://doi.org/10.1016/S0921-5093(00)01892-X)
46. J. Kopeček et al., Ordering in the sublattices of Fe₃Al during the phase transformation B2–D0₃. *Intermetallics* **7**(12), 1367–1372 (1999). doi:[10.1016/S0966-9795\(99\)00057-6](https://doi.org/10.1016/S0966-9795(99)00057-6)
47. M. Kogachi, T. Haraguchi, S.M. Kim, Point defect behavior in high temperature region in the B2-type intermetallic compound FeAl. *Intermetallics* **6**(6), 499–510 (1998). doi:[10.1016/S0966-9795\(97\)00097-6](https://doi.org/10.1016/S0966-9795(97)00097-6)
48. W. Köster, T.Gödecke, Physical measurements on iron-aluminum alloys between 10 and 50 at. % Al. *Zeitschrift fuer Metallkunde* **71**, 765 (1980)
49. R. Krachler et al., Diffusion mechanism and defect concentrations in β'-FeAl, an intermetallic compound with B2 structure. *Intermetallics* **3**(1), 83–88 (1995). doi:[10.1016/0966-9795\(94\)P3690-P](https://doi.org/10.1016/0966-9795(94)P3690-P)

50. R. Krachler, H. Ipser, K.L. Komarek, Thermodynamics of intermetallic B2-phases. A generalized model. *J. Phys. Chem. Solids* **50**(11), 1127–1135 (1989). doi:[10.1016/0022-3697\(89\)90022-X](https://doi.org/10.1016/0022-3697(89)90022-X)
51. F. Král, P. Schwander, G. Kostorz, Superdislocations and antiphase boundary energies in deformed Fe₃Al single crystals with chromium. *Acta Mater.* **45**(2), 675–682 (1997). doi:[10.1016/S1359-6454\(96\)00181-4](https://doi.org/10.1016/S1359-6454(96)00181-4)
52. O. Kubashewski, *Iron Binary Diagrams* (Springer, Berlin, 1982)
53. M. Kupka, Can vacancies be the main reason of FeAl alloys hardening? *J. Alloys Compd.* **437**(1–2), 373–377 (2007). doi:[10.1016/j.jallcom.2006.12.013](https://doi.org/10.1016/j.jallcom.2006.12.013)
54. H. Lai et al., Etude couplée calorimétrique et dilatométrique de l'enthalpie d'élimination des lacunes de trempe lors du revenu d'alliages ordonnés B2 Fe_{50+x}Al_{50-x} (–1 < x < 10). *Acta Metall.* **34**(3), 425–436 (1986). doi:[10.1016/0001-6160\(86\)90078-7](https://doi.org/10.1016/0001-6160(86)90078-7)
55. A. Lawley, R.W. Cahn, A high temperature X-ray study of ordering in iron-aluminium alloys. *J. Phys. Chem. Solids* **20**(3–4), 204–221 (1961). doi:[10.1016/0022-3697\(61\)90007-5](https://doi.org/10.1016/0022-3697(61)90007-5)
56. G. Lütjering, H. Warlimont, Ordering of Fe₃Al and Cu₃Al by first order transformations. *Acta Metall.* **12**(12), 1460–1461 (1964). doi:[10.1016/0001-6160\(64\)90138-5](https://doi.org/10.1016/0001-6160(64)90138-5)
57. M.J. Marcinkowski, N. Brown, Theory and direct observation of dislocations in the Fe₃Al superlattices. *Acta Metall.* **9**(8), 764–786 (1961). doi:[10.1016/0001-6160\(61\)90107-9](https://doi.org/10.1016/0001-6160(61)90107-9)
58. M.J. Marcinkowski, N. Brown, Direct observation of antiphase boundaries in the Fe₃Al superlattice. *J. Appl. Phys.* **33**(2), 537–552 (1962). doi:[10.1063/1.1702463](https://doi.org/10.1063/1.1702463)
59. M.G. Mendiratta, H.-M. Kim, H.A. Lipsitt, Slip directions in B2 Fe-Al alloys. *Metall. Trans. A* **15**(2), 395–399 (1984). doi:[10.1007/BF02645127](https://doi.org/10.1007/BF02645127)
60. M. Mihalkovč, M. Widom, Structure and stability of Al₂Fe and Al₅Fe₂: first-principles total energy and phonon calculations. *Phys. Rev. B* **85**(1), 014113 (2012). doi:[10.1103/PhysRevB.85.014113](https://doi.org/10.1103/PhysRevB.85.014113)
61. A.M. Moisin, L.H. Moisin, Short range order investigation by neutron scattering. *Solid State Commun.* **21**(5), 413–415 (1977). doi:[10.1016/0038-1098\(77\)91363-1](https://doi.org/10.1016/0038-1098(77)91363-1)
62. D. Morris, M. Morris, Strengthening at intermediate temperatures in iron aluminides. *Mater. Sci. Eng. A* **239–240**(0), 23–38 (1997). doi:[10.1016/S0921-5093\(97\)00557-1](https://doi.org/10.1016/S0921-5093(97)00557-1)
63. D.G. Morris, M.A. Munoz-Morris, The stress anomaly in FeAl-Fe₃Al alloys. *Intermetallics* **13**(12), 1269–1274 (2005). doi:[10.1016/j.intermet.2004.08.012](https://doi.org/10.1016/j.intermet.2004.08.012)
64. D. Morris, M. Muñoz-Morris, A re-examination of the pinning mechanisms responsible for the stress anomaly in FeAl intermetallics. *Intermetallics* **18**(7), 1279–1284 (2010). doi:[10.1016/j.intermet.2009.12.021](https://doi.org/10.1016/j.intermet.2009.12.021)
65. J.P. Neumann, On the occurrence of substitutional and triple defects in intermetallic phases with the B2 structure. *Acta Metall.* **28**(8), 1165–1170 (1980). doi:[10.1016/0001-6160\(80\)90099-1](https://doi.org/10.1016/0001-6160(80)90099-1)
66. J.P. Neumann, Y.A. Chang, C.M. Lee, Thermodynamics of intermetallic phases with the triple-defect B2 structure. *Acta Metall.* **24**(7), 593–604 (1976). doi:[10.1016/0001-6160\(76\)90078-X](https://doi.org/10.1016/0001-6160(76)90078-X)
67. K. Oki, M. Hasaka, T. Eguchi, X-ray diffraction study of kinetic behaviours of ordering in Fe₃Al alloy. *Trans. Jpn. Inst. Met.* **14**(1), 8–14 (1973)
68. D. Paris, P. Lesbats, Vacancies in Fe-Al alloys. *J. Nucl. Mater.* **69**(70), 628–632 (1978). doi:[10.1016/0022-3115\(78\)90297-0](https://doi.org/10.1016/0022-3115(78)90297-0)
69. L.M. Pike et al., Site occupancies, point defect concentrations, and solid solution hardening in B2 (Ni, Fe)Al. *Acta Mater.* **50**(15), 3859–3879 (2002). doi:[10.1016/S1359-6454\(02\)00192-1](https://doi.org/10.1016/S1359-6454(02)00192-1)
70. L.M. Pike, Y.A. Chang, C.T. Liu, Point defect concentrations and hardening in binary B2 intermetallics. *Acta Mater.* **45**(9), 3709–3719 (1997). doi:[10.1016/S1359-6454\(97\)00028-1](https://doi.org/10.1016/S1359-6454(97)00028-1)
71. V. Pierron-Bohnes et al., Short range order in a single crystal of Fe-19.5 at.% Al in the ferromagnetic range measured through X-ray diffuse scattering. *Acta Metall. Mater.* **38**(12), 2701–2710 (1990). doi:[10.1016/0956-7151\(90\)90284-N](https://doi.org/10.1016/0956-7151(90)90284-N)
72. X. Ren, K. Otsuka, M. Kogachi, Do "constitutional vacancies" in intermetallic compounds exist? *Scr. Mater.* **41**(9), 907–913 (1999). doi:[10.1016/S1359-6462\(99\)00235-3](https://doi.org/10.1016/S1359-6462(99)00235-3)

73. L. Rimlinger, B. Faivre, Contribution de la microscopie electronique a fond noir a l'établissement du diagramme de transformation des alliages fer-aluminium riches en fer. *J. Nucl. Mater.* **28**(2), 211–214 (1968). doi:[10.1016/0022-3115\(68\)90028-7](https://doi.org/10.1016/0022-3115(68)90028-7)
74. J.P. Rivière, J. Grilhé, Restauration de défauts de trempe dans un alliage Fe-Al 40 at.% ordonné. *Acta Metall.* **20**(11), 1275–1280 (1972). doi:[10.1016/0001-6160\(72\)90058-2](https://doi.org/10.1016/0001-6160(72)90058-2)
75. J.P. Rivière, J. Grilhé, Energie de formation des lacunes dans les alliages Fe-Al ordonnés de type B2. *Scr. Metall.* **9**(9), 967–970 (1975). doi:[10.1016/0036-9748\(75\)90553-0](https://doi.org/10.1016/0036-9748(75)90553-0)
76. J.P. Riviere, Structural defects in β phase Fe-Al. *Mater. Res. Bull.* **12**(10), 995–1000 (1977). doi:[10.1016/0025-5408\(77\)90024-1](https://doi.org/10.1016/0025-5408(77)90024-1)
77. H. Rösner et al., Tensile tests of $\text{Fe}_{70}\text{Al}_{30}$ in a TEM in the temperature range of the yield stress anomaly. *Mater. Sci. Eng. A* 192–193, Part 2.0, 793–798 (1995). doi:[10.1016/0921-5093\(94\)03316-1](https://doi.org/10.1016/0921-5093(94)03316-1)
78. H. Sagane, K. Oki, T. Eguchi, Observation of phase separation in Fe_3Al alloys. *Trans. Jpn. Inst. Met.* **18** (1977)
79. H. Saitô, H. Morita, On the nature of the K-state in the system of iron and aluminium. *J. Jpn. Inst. Met.* **30**(10), 930–935 (1966)
80. H.-E. Schaefer, K. Frenner, R. Wurschum, Time-differential length change measurements for thermal defect investigations: intermetallic B2-FeAl and B2-NiAl compounds, a case study. *Phys. Rev. Lett.* **82**(5), 948–951 (1999). doi:[10.1103/PhysRevLett.82.948](https://doi.org/10.1103/PhysRevLett.82.948)
81. H.-E. Schaefer et al., Thermal vacancies and positron-lifetime measurements in $\text{Fe}_{76.3}\text{Al}_{23.7}$. *Phys. Rev. B* **41**(17), 11869–11874 (1990). doi:[10.1103/PhysRevB.41.11869](https://doi.org/10.1103/PhysRevB.41.11869)
82. J.H. Schneibel, L.M. Pike, A technique for measuring thermal vacancy concentrations in stoichiometric FeAl. *Intermetallics* **12**(1), 85–90 (2004). doi:[10.1016/j.intermet.2003.09.003](https://doi.org/10.1016/j.intermet.2003.09.003)
83. W. Schweika, Difuse neutron scattering study of short-range order in $\text{Fe}_{0.8}\text{Al}_{0.2}$ alloy, In: *MRS Online Proceedings Library*, vol. 166, (1989). doi:[10.1557/PROC-166-249](https://doi.org/10.1557/PROC-166-249)
84. O. Seménova, R. Krachler, H. Ipser, A generalized defect correlation model for B2 compounds. *Solid State Sci.* **10**(9), 1236–1244 (2008). doi:[10.1016/j.solidstatesciences.2007.11.041](https://doi.org/10.1016/j.solidstatesciences.2007.11.041)
85. F. Stein, A. Schneider, G. Frommeyer, Flow stress anomaly and order-disorder transitions in Fe_3Al -based Fe-Al-Ti-X alloys with X=V, Cr, Nb, or Mo. *Intermetallics* **11**(1), 71–82 (2003). doi:[10.1016/S0966-9795\(02\)00187-5](https://doi.org/10.1016/S0966-9795(02)00187-5)
86. F. Stein et al., Determination of the crystal structure of the ε phase in the Fe-Al system by high-temperature neutron diffraction. *Intermetallics* **18**(1), 150–156 (2010). doi:[10.1016/j.intermet.2009.07.006](https://doi.org/10.1016/j.intermet.2009.07.006)
87. N.S. Stolof, R.G. Davies, The plastic deformation of ordered FeCo and Fe_3Al alloys. *Acta Metall.* **12**(5), 473–485 (1964). doi:[10.1016/0001-6160\(64\)90019-7](https://doi.org/10.1016/0001-6160(64)90019-7)
88. B. Sundman et al., An assessment of the entire Al-Fe system including DO_3 ordering. *Acta Mater.* **57**(10), 2896–2908 (2009). doi:[10.1016/j.actamat.2009.02.046](https://doi.org/10.1016/j.actamat.2009.02.046)
89. P.R. Swann, R.M. Fisher, Effect of magnetization on the L_{20} ordering reaction in iron-aluminum alloys. *Appl. Phys. Lett.* **9**(8), 279–281 (1966). doi:[10.1063/1.1754749](https://doi.org/10.1063/1.1754749)
90. G. Taylor, Thermally-activated deformation of BCC metals and alloys. *Prog. Mater. Sci.* **36**, 29–61 (1992). doi:[10.1016/0079-6425\(92\)90004-Q](https://doi.org/10.1016/0079-6425(92)90004-Q)
91. A. Taylor, R.M. Jones, Constitution and magnetic properties of iron rich iron-aluminum alloys. *J. Phys. Chem. Solids* **6**(1), 16–37 (1958). doi:[10.1016/0022-3697\(58\)90213-0](https://doi.org/10.1016/0022-3697(58)90213-0)
92. H. Thomas, Über Widerstandslegierungen. *Zeitschrift für Physik* **129**(2), 219–232 (1951). doi:[10.1007/BF01333398](https://doi.org/10.1007/BF01333398)
93. Y. Umakoshi, M. Yamaguchi, Deformation of FeAl single crystals at high temperatures. *Philos. Mag. A* **41**(4), 573–588 (1980). doi:[10.1080/01418618008239334](https://doi.org/10.1080/01418618008239334)
94. V. Vitek, Structure of dislocation cores in metallic materials and its impact on their plastic behaviour. *Prog. Mater. Sci.* **36**, 1–27 (1992). doi:[10.1016/0079-6425\(92\)90003-P](https://doi.org/10.1016/0079-6425(92)90003-P)
95. V. Vitek, V. Paidar, Non-planar dislocation cores: a ubiquitous phenomenon affecting mechanical properties of crystalline materials, in *Dislocations in Solid*, vol. 14, ed. by J.P. Hirth (Elsevier, 2008), pp. 439–514
96. V. Volterra, Sur l'équilibre des corps elastiques multiplement connexes. *Annales scientifiques de l'École Normale Supérieure* **24**, 401–517 (1907)

97. D. Watanabe et al., Transmission electron microscopic study on the "K-State" in iron-aluminium alloys. *J. Phys. Soc. Jpn.* **29**(3), 722–729 (1970). doi:[10.1143/JPSJ.29.722](https://doi.org/10.1143/JPSJ.29.722)
98. R. Würschum, C. Grupp, H.-E. Schaefer, Simultaneous study of vacancy formation and migration at high temperatures in B2-Type Fe aluminides. *Phys. Rev. Lett.* **75**(1), 97–100 (1995). doi:[10.1103/PhysRevLett.75.97](https://doi.org/10.1103/PhysRevLett.75.97)
99. H. Xiao, I. Baker, The temperature dependence of the flow and fracture of Fe-40Al. *Scr. Metall. Mater.* **28–11**, 1411–1416 (1993). doi:[10.1016/0956-716X\(93\)90491-A](https://doi.org/10.1016/0956-716X(93)90491-A)
100. H. Xiao, I. Baker, The relationship between point defects and mechanical properties in Fe-Al at room temperature. *Acta Metall. Mater.* **43**(1), 391–396 (1995). doi:[10.1016/0956-7151\(95\)90295-3](https://doi.org/10.1016/0956-7151(95)90295-3)
101. K. Yoshimi, S. Hanada, The strength properties of iron aluminides. *JOM* **49**(8), 46–49 (1997). doi:[10.1007/BF02914403](https://doi.org/10.1007/BF02914403)
102. K. Yoshimi, S. Hanada, M.H. Yoo, Yielding and plastic flow behavior of B2-type Fe-39.5 mol. % Al single crystals in compression. *Acta Metallurgica et Materialia Metallurgica et Materialia* **43**(11), 4141–4151 (1995). doi:[10.1016/0956-7151\(95\)00098-G](https://doi.org/10.1016/0956-7151(95)00098-G)
103. S. Zuqing et al., Neutron diffraction study on site occupation of substitutional elements at sub lattices in Fe₃Al intermetallics. *Mater. Sci. Eng. A* **258**(1–2), 69–74 (1998). doi:[10.1016/S0921-5093\(98\)00919-8](https://doi.org/10.1016/S0921-5093(98)00919-8)

Nanoscale AFM and TEM Observations of Elementary
Dislocation Mechanisms

Veselý, J.

2017, XIV, 100 p. 86 illus., 21 illus. in color., Hardcover

ISBN: 978-3-319-48301-6